Geophysical Research Letters

RESEARCH LETTER
10.1029/2018GL078206

**Key Points:**
- High-latitude field-aligned currents and equatorial plasma flows are observed within the same flux tube
- Field-aligned current intensity is well correlated with the magnitude of tailward equatorial plasma flows
- Near-Earth reconnection is an important trigger of field-aligned currents observed at the plasma sheet boundary

**Supporting Information:**
- Supporting Information S1

**Correspondence to:**
A. V. Artemyev,
aartemyev@igpp.ucla.edu

**Citation:**
Artemyev, A. V., Pritchett, P. L., Angelopoulos, V., Zhang, X.-J., Nakamura, R., Lu, S., et al. (2018). Field-aligned currents originating from the magnetic reconnection region: Conjugate MMS-ARTEMIS observations. *Geophysical Research Letters*, *45*, 5836–5844. https://doi.org/10.1029/2018GL078206

Received 6 APR 2018
Accepted 6 JUN 2018
Accepted article online 14 JUN 2018
Published online 28 JUN 2018



# Field-Aligned Currents Originating From the Magnetic Reconnection Region: Conjugate MMS-ARTEMIS Observations

**A. V. Artemyev[1,2], P. L. Pritchett[3], V. Angelopoulos[1], X.-J. Zhang[1], R. Nakamura[4], S. Lu[1], A. Runov[1], S. A. Fuselier[5], S. Wellenzohn[4], F. Plaschke[4], C. T. Russell[1], R. J. Strangeway[1], P.-A. Lindqvist[6], and R. E. Ergun[7]**

[1]Department of Earth, Planetary, and Space Sciences and Institute of Geophysics and Planetary Physics, University of California, Los Angeles, CA, USA, [2]Space Research Institute, RAS, Moscow, Russia, [3]Department of Physics and Astronomy, University of California, [4]Space Research Institute, Austrian Academy of Sciences, Graz, Austria, [5]Southwest Research Institute, San Antonio, TX, USA, [6]Royal Institute of Technology, Stockholm, Sweden, [7]LASP, University of Colorado Boulder, Boulder, CO, USA

**Abstract** Near-Earth magnetic reconnection reconfigures the magnetotail and produces strong plasma flows that transport plasma sheet particles and electromagnetic energy to the inner magnetosphere. An essential element of such a reconfiguration is strong, transient field-aligned currents. These currents, believed to be generated within the plasma sheet and closed at the ionosphere, are responsible for magnetosphere-ionosphere coupling during substorms. We use conjugate measurements from Magnetospheric Multiscale (MMS) at the plasma sheet boundary (around $x \sim -10R_E$) and Acceleration, Reconnection, Turbulence and Electrodynamics of the Moon's Interaction with the Sun (ARTEMIS) at the equator (around $x \sim -60R_E$) to explore the potential generation region of these currents. We find a clear correlation between the field-aligned current intensity measured by MMS and the tailward plasma sheet flows measured by ARTEMIS. To better understand the origin of this correlation, we compare spacecraft observations with results from 3-D particle-in-cell simulations of magnetotail reconnection. The comparison reveals that field-aligned currents and plasma flows start, wax, and wane due to the development of a reconnection region between MMS (near-Earth) and ARTEMIS (at lunar distance). A weak correlation between the field-aligned current intensity at MMS and earthward flow magnitudes at ARTEMIS suggests that distant magnetotail reconnection does not significantly contribute to the generation of the observed near-Earth currents. Our findings support the idea that the dominant role of the near-Earth magnetotail reconnection in the field-aligned current generation is likely responsible for their transient nature, whereas more steady distant tail reconnection would support long-term field-aligned current system.

**Plain Language Summary** Field-aligned currents connect the Earth magnetotail and ionosphere, proving energy and information transport from the region where main energy release process, magnetic reconnection, occurs to the region where the collisional energy dissipation takes place. Therefore, investigation and modeling of the field-aligned current generation is important problem of the magnetosphere plasma physics. However, field-aligned current investigation requires simultaneous observations of reconnection signatures in the magnetotail and at high latitudes. Simultaneous and conjugate operation of two multispacecraft missions, Magnetospheric Multiscale and Acceleration, Reconnection, Turbulence and Electrodynamics of the Moon's Interaction with the Sun, for the first time provide an opportunity for such investigation. Combining spacecraft observations with results from 3-D particle-in-cell simulations of magnetotail reconnection, we demonstrate that field-aligned currents and plasma flows start, wax, and wane due to the development of a reconnection region between near-Earth (Magnetospheric Multiscale location) and lunar distant tail (Acceleration, Reconnection, Turbulence and Electrodynamics of the Moon's Interaction with the Sun location). Our findings support the idea that the dominant role of the near-Earth magnetotail reconnection in the field-aligned current generation is likely responsible for their transient nature, whereas more steady distant tail reconnection would support long-term field-aligned current system.

## 1. Introduction

Energy release caused by magnetic reconnection, one of the most powerful plasma heating processes in the Earth's magnetotail, is responsible for magnetotail reconfiguration and many highly energetic phenomena (e.g., Angelopoulos et al., 2008; Baker et al., 1996). Near the reconnection site, some of the released magnetic energy is transformed into plasma acceleration and heating; the remainder is transported toward the near-Earth region by equatorial plasma flows and field-aligned currents (see review by Paschmann et al., 2013, and references therein). Numerous spacecraft observations in the equatorial magnetotail have provided us with detailed information on accelerated plasma flows and plasma heating caused by reconnection (e.g., Angelopoulos et al., 2013; Chaston et al., 2014; Eastwood et al., 2013; Nagai et al., 2013; Tyler et al., 2016, and references therein). Much less is known about field-aligned currents that originate at the reconnection region, however, because their detailed investigation requires simultaneous observations of equatorial and high-latitude reconnection signatures (see, e.g., examples of such observations in Angelopoulos et al., 2002; Nakamura et al., 2017; Varsani et al., 2017).

The simultaneous presence of Magnetospheric Multiscale (MMS) (Burch et al., 2016) and Acceleration, Reconnection, Turbulence and Electrodynamics of the Moon's Interaction with the Sun (ARTEMIS; Angelopoulos, 2011) in the magnetotail provides a unique opportunity to conduct statistical investigations of the relationship between equatorial and high-latitude nightside signatures of near-Earth magnetic reconnection. We employ four-spacecraft analysis techniques at MMS (e.g., Dunlop et al., 2002) to determine field-aligned currents at the near-Earth (below ~15 Earth radii, $R_E$) plasma sheet boundary. In section 2, we selected such MMS events which were conjugate with equatorial ARTEMIS observations in the magnetotail at lunar (~60 $R_E$) distances. To establish such MMS-ARTEMIS conjunctions, we examined ion density and temperature measurements at two spacecraft (previous simulations and observations [see Lu et al., 2017] have demonstrated that not only the density but also the ion temperature is conserved along magnetic field lines; thus, we use the agreement in ion density and temperature as a proxy of field-line mapping between the two spacecraft). Times were first selected when the separation between MMS and ARTEMIS along the dawn-dusk direction was small ($\leq$5 $R_E$) and the spacecraft measured similar plasma temperatures and densities. We then compared field-aligned currents measured by MMS at the plasma sheet boundary to plasma flows measured by ARTEMIS near the equator to investigate the relationship between high-latitude and equatorial signatures of near-Earth magnetic reconnection (see pictorial representation in Figure 1).

To further investigate whether field-aligned currents and equatorial plasma flows are generated by the same source, in section 3 we turned to 3-D particle-in-cell (PIC) simulations of magnetic reconnection in a realistic magnetotail configuration that includes a current sheet and the dipole field (Pritchett, 2015; Pritchett & Runov, 2017). Comparisons of the simulation results and MMS/ARTEMIS measurements provide an interpretational basis in a global context for observations of magnetotail dynamics driven by magnetic reconnection. Such comparisons guide our observational questions to test our ideas of the field-aligned current origin.

## 2. MMS and ARTEMIS Observations

Obtaining conjugate spacecraft measurements at the plasma sheet boundary and in the equatorial region requires first and foremost that ARTEMIS and MMS be in the nightside magnetotail close to one another in dawn-dusk coordinates. Every month, ARTEMIS P1 and P2 spend about 3 days within the magnetotail (Angelopoulos, 2011); MMS spent 5 months from May to September in 2016 and 2017 in the nightside magnetosphere (frequently encountering the plasma sheet boundary during those times).

From this time interval we selected nine events that satisfy the following criteria (see event list in the supporting information): (1) spacecraft separation (MMS and ARTEMIS) along the dawn-dusk direction is within 5 $R_E$ (the maximum size of the plasma flow originating from magnetotail reconnection, see Li et al., 2014; Nakamura et al., 2004); (2) ARTEMIS spacecraft are in the plasma sheet (i.e., during those times crossing $B_x = 0$, as measured by the Fluxgate Magnetometer, see Auster et al., 2008); (3) the magnetic field $|B_x|$ decreases (interpreted as plasma sheet expansion during dipolarization) at MMS (magnetic fields are measured by the MMS magnetometers, see Russell et al., 2016) as the electric field exhibits bursts of large amplitude (electric fields are measured by the FIELDS Instrument Suite on MMS, see Ergun et al., 2016; Torbert et al., 2016); (4) ARTEMIS equatorial ion temperature $T_i$ and density $n_i$ (measured by the Electrostatic Analyser, see McFadden et al., 2008) are comparable to those measured by MMS (by Hot Plasma Composition Analyzer, HPCA, see Young et al., 2016) at the plasma sheet boundary before the dipolarization. Note that we used HPCA

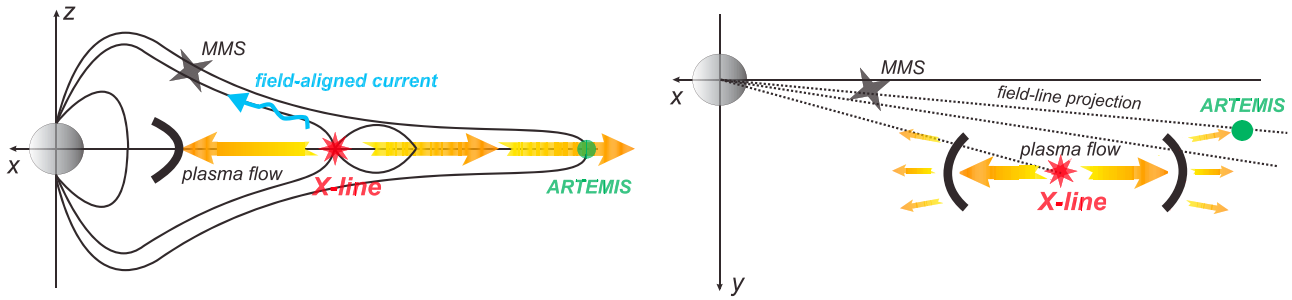


**Figure 1.** Schematic view of Magnetospheric Multiscale (MMS) and Acceleration, Reconnection, Turbulence and Electrodynamics of the Moon's Interaction with the Sun (ARTEMIS) observations of magnetotail reconnection in $(x, z)$ plane (left panel) and $(x, y)$ plane (right panel).

ion measurements (total proton and oxygen densities and the average temperature) because HPCA was the only MMS plasma instrument operating at the near-Earth plasma sheet boundary in 2016. In the absence of HPCA data, we use the electron density derived from the spacecraft potential (Andriopoulou et al., 2016) to compare with ARTEMIS equatorial plasma measurements. (Note that a similar ion temperature and/or electron density measured by ARTEMIS and MMS can definitely confirm that spacecraft are within the same flux tube only in an idealistic static magnetotail configuration, whereas in the realistic dynamical magnetotail these measurements suggest that spacecraft are located at close flux tubes). Our events are terminated by the rapid $|B_x|$ decrease at MMS, signifying dipolarization in the aftermath of reconnection further downtail from those spacecraft. The events are selected to start tens of minutes to hours prior to that decrease, signifying prolonged residence of MMS near the quasi-static plasma sheet boundary, as expected during substorm growth phase or quiet times.

We show one event from nine in Figure 2. Panel (a) shows magnetic fields measured by ARTEMIS P1, P2, and MMS-1 during an ~2-hr interval (ARTEMIS and MMS separation along the dawn-dusk direction is within a few $R_E$ for the entire interval, see panel (d)). The gray box shows near-equatorial ARTEMIS measurements, and the blue box shows the rapid $|B_x|$ decrease (the dipolarization) observed by MMS. Before the dipolarization, MMS, at the plasma sheet boundary, measured $T_i$ comparable to that at ARTEMIS (see Figure 2b). Plotted versus the magnetic field, the ion temperatures measured by MMS and ARTEMIS, $T_i(B_x)$, exhibit typical (Artemyev et al., 2017; Lu et al., 2017, and references therein) bell-shaped profiles (see Figure 2e). The peak (equatorial) value of ARTEMIS $T_i$ is comparable to the lowest (boundary layer) MMS $T_i$, from which we can conclude that ARTEMIS and MMS are located approximately on the same flux tube. Figure 3c shows that during the entire interval, ARTEMIS observed significant (>400 km/s, compared to the thermal speed of ~400 km/s) bursts of plasma flows (both earthward, $v_x > 0$, and tailward, $v_x < 0$), which became especially strong when MMS observed the $|B_x|$ decrease (dipolarization) and electric field bursts (black trace in Figure 2c). Figure 2f shows the current density at MMS. A burst of strong (mostly field aligned) currents was detected by MMS during the dipolarization. Although the current density is averaged over ~3 s to smooth very intense currents likely produced by Alfven wave activity (e.g., Wygant et al., 2002), even such smoothed current density reaches ~50 nA/m$^2$.

The behavior of the conjunction event in Figure 2 is typical of the others in our database. Tailward flows at ARTEMIS prior to (or during) MMS dipolarization can be interpreted as small-scale (azimuthally localized) and low-intensity activations of the near-Earth reconnection. Azimuthally localized flows can set nearby plasma into motion, transferring momentum via vortices and cross-field diffusion across the plasma sheet (in $y$, see scheme in Figure 1). The resultant flows observed at ARTEMIS reach 500–1,000 km/s just before dipolarization (observed by MMS), which we interpret as evidence for the activation of near-Earth reconnection, at or near the MMS-ARTEMIS line (for six events out of nine, the peak ion velocity at ARTEMIS is tailward). Because this is due to short-lived ARTEMIS flows, it does not invalidate the MMS-ARTEMIS mapping argument prior to reconnection onset, which was established by comparing ion density and temperature data collected prior to the MMS dipolarization (dominated by the slow-flow regime).

To statistically relate plasma flows to field-aligned currents for the events collected, we compare the average $j_\parallel$ over the ±5-min interval around $j_\parallel$ maximum with the average $v_x$ estimated in the following way. Because many transient plasma flows were measured by ARTEMIS before the dipolarization detection by MMS, to characterize these flows, we separately average $v_x < -100$ km/s (tailward flows) and $v_x > 100$ km/s (earthward flows) over ~ ±20 min around the MMS dipolarization. For some events, ARTEMIS P1 and P2 are not

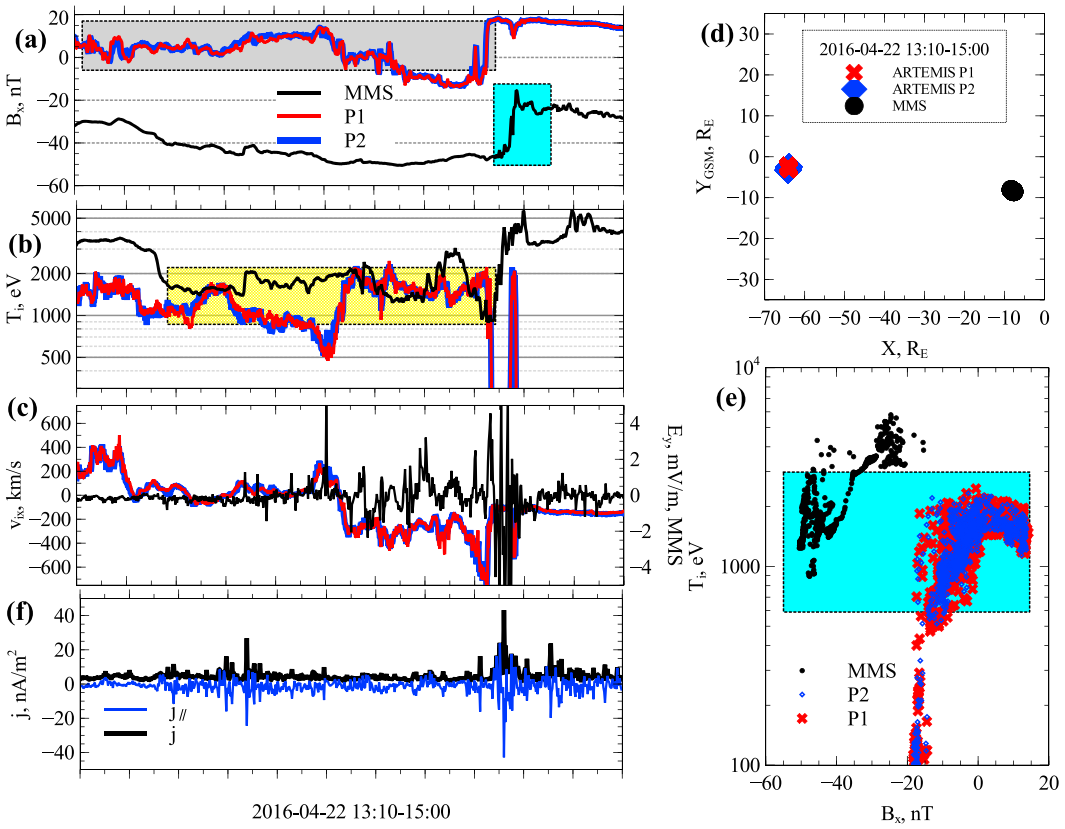


**Figure 2.** One event from our data set. Panel (a) shows magnetic field measured by Magnetospheric Multiscale (MMS; the plasma sheet boundary) and Acceleration, Reconnection, Turbulence and Electrodynamics of the Moon's Interaction with the Sun (ARTEMIS; the equatorial plane). The gray box indicates ARTEMIS P1 and P2 equatorial measurements; the blue box shows the dipolarization (the $|B_x|$ decrease) observed by MMS. Panel (b) shows ion temperatures measured by MMS and ARTEMIS. The yellow box shows the time interval during which MMS and ARTEMIS measurements provided the same temperature. Panel (c) shows equatorial plasma flows (ARTEMIS) and electric field GSM $E_y$ measured at the plasma sheet boundary (MMS). Panel (d) shows the positions of the MMS and ARTEMIS spacecraft in the $(x, y)$ GSM plane. Panel (e) shows ion temperature distributions across the magnetotail, $T_i(B_x)$. The blue box shows similar temperatures measured by MMS and ARTEMIS. Panel (f) shows the current density (total $|\mathbf{j}|$ and field-aligned $j_{||}$) calculated using MMS four-point magnetic field measurements.

always around the equatorial plane, $B_x \sim 0$. To exclude field-aligned cold ion steams flowing in the plasma sheet boundary, which we interpret as mantle plasma or the effect of reconnection much further downtail than ARTEMIS, instead of local neutral sheet activations, we calculate averaged $v_x$ only when $|B_x| < 10$ nT in the aforementioned time interval. Although such averaged $v_x$ does not always correspond temporally to the field-aligned currents measured during the $\sim$ 10-min interval at MMS, it reveals the general intensity of tailward and earthward plasma flows before (and during) the near-Earth dipolarizations. For each event we consider earthward or tailward ion $v_x$ (whichever is larger) and compare it with filed-aligned current magnitudes measured by MMS.

Previous simulations and observations (see, e.g., Birn & Hesse, 2013; Kepko et al., 2014, and references therein) suggest that the field-aligned current intensity should depend on the intensity of equatorial plasma flows at the conjugate location. Our result (Figure 3) confirms this: the intensity of MMS-measured field-aligned currents is indeed proportional to the average magnitude of tailward plasma flows measured by ARTEMIS (during six out of nine events). However, there is no clear correlation between field-aligned currents and earthward flows for the other three events when these flows dominate over tailward flows. This suggests that the near-Earth dipolarization and the accompanying field-aligned currents were likely triggered by magnetic reconnection between MMS and ARTEMIS but not tailward of ARTEMIS. We should note that although MMS and ARTEMIS were (by event-selection) located within the same flux tube prior to the onset of strong near-Earth reconnection activity, the intense currents measured by MMS were likely not generated at ARTEMIS

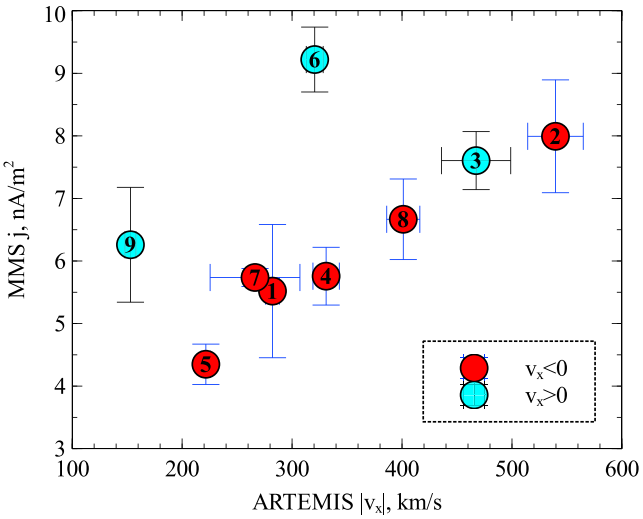


**Figure 3.** The average intensity of field-aligned currents (Magnetospheric Multiscale, MMS) versus the average magnitude of equatorial plasma flows (Acceleration, Reconnection, Turbulence and Electrodynamics of the Moon's Interaction with the Sun, ARTEMIS) for nine events. Numbers within circles correspond to event numbers as listed in the supporting information.

(since there is no evidence of reconnection there), but rather earthward of it, at the near-Earth neutral line. To further explore this hypothesis, we compare patterns seen in the observational data with results of numerical simulations.

## 3. Three-Dimensional PIC Simulations

We analyze the results of a 3-D PIC simulation that retains the full dynamics for both electrons and ions (see details of code in Pritchett et al., 1996). The initial near-Earth magnetotail configuration consists of the current sheet model (Lembege & Pellat, 1982) and the vacuum field of a line (2D) dipole field. Details of the simulation setup, the initial and boundary conditions, and the reconnection initialization can be found in Pritchett et al. (1991), Pritchett and Coroniti (1998), and (Pritchett, 2015).

Figures 4a–4c show simulation results of 2-D spatial distributions of earthward-tailward ion flows, field-aligned currents, and plasma density, respectively, in the $(x, z)$ plane. These distributions are plotted for a particular $y$ slice of the 3-D simulation box, at $y = 0$. The magnetic reconnection region at $x \sim 0$ is the origin of plasma flows propagating in both directions (tailward and earthward; Earth is located on the left, as the simulation $x$ coordinate has the opposite sign to that of GSM $x$). We use two $x = const$ cuts to examine the $z$ profiles of various plasma parameters (located at the two dashed vertical lines depicted in each of Figures 4a–4c). Shown in Figures 4d–4g are the $z$ profiles of density and current density at four select times during the simulations.

Comparison of the $z$ profiles of the density (Figures 4d and 4e) shows that the equatorial density at the tailward side of the reconnection site, at a location consistent with the virtual position of ARTEMIS ($z = 0$, $x = 25d_i$), is approximately equal to the density at the earthward plasma sheet boundary layer, at a location consistent with the virtual position of MMS ($z \in [-3, -5]d_i$ at $x = -50d_i$). Note that to compare spacecraft locations in the context of PIC simulations, we used the ion density, whereas in observations we also used the ion temperature. We did this because the density controls the plasma pressure distribution for the simulation setup (see properties of the initial current sheet model in Lembege & Pella, 1982), whereas the temperature variations contribute more to the pressure distribution in the magnetotail (e.g., Artemyev et al., 2017). The virtual positions of ARTEMIS and MMS in physical space cannot be directly compared to the simulation scales. Rather, in the context of simulations, we simply chose an ARTEMIS $x$ location in the tailward outflow region and then elected the MMS $x$ coordinate to be symmetric on the earthward side of reconnection and the $z$ coordinate such that MMS is conjugate to ARTEMIS based on observing the same density prior to the onset of reconnection.

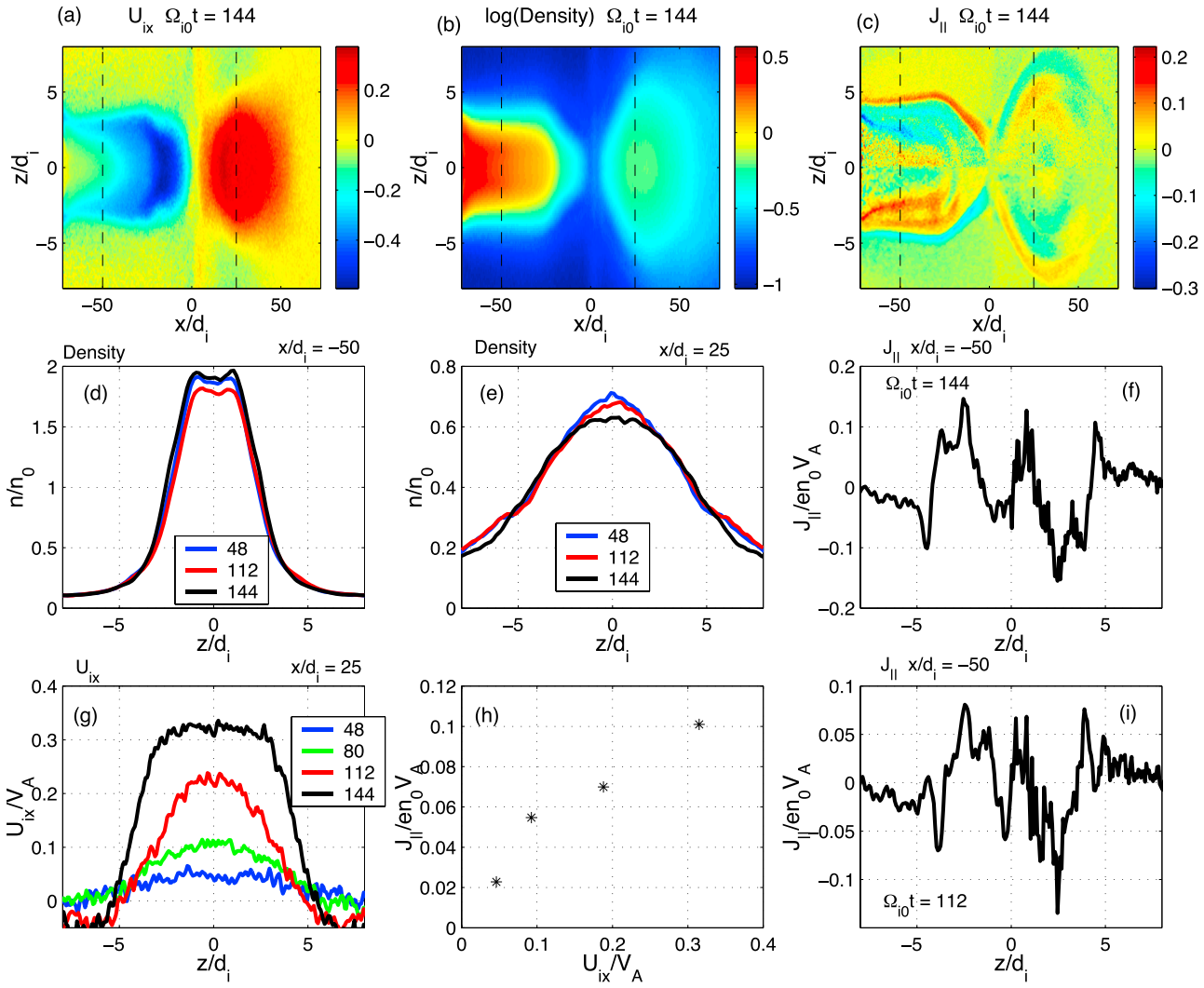


**Figure 4.** Results of the numerical simulation of 3-D magnetic reconnection in the realistic magnetotail configuration. Panels (a–c) show $(x, z)$ distributions of plasma flows, plasma density, field-aligned currents. These 2-D slices at $y \approx 0$ are plotted for time $t = 144\Omega_{0i}^{-1}$. Two black vertical dashed lines indicate the positions for collection of $z$ profiles shown in panels (d–g) for different time moments. Average values of ion flow velocity in the plasma sheet, $z \in [-3, 3]d_i$, from panel (g) and peak values of field-aligned currents (for $z \in [-5, -3]d_i$) from panels (f), (i), and two other times are shown in panel (h). The plasma density is normalized to the initial peak value of the current sheet plasma density, $n_0$; the ion flow velocity is normalized to the Alfven speed $v_A = B_0/\sqrt{4\pi n_0 m_p}$, where $B_0$ is the initial peak value of the lobe current sheet $B_x$ field (used for $\Omega_{0i}$ calculation as well); the field-aligned current is normalized to $en_0v_A$ (see details in Pritchett, 2015).

Strong field-aligned currents form around the virtual MMS position ($x = -50d_i, z \sim -4d_i$; see Figures 4f and 4i). To characterize these currents, we use the negative peak value of $j_{||}$ (earthward in simulation coordinates) around $z \sim -4d_i$. Figure 4g shows the $z$ profiles of the ion flow velocity at the virtual ARTEMIS position. The velocity gradually increases during the simulation; thus, we can compare $v_x(t)$ (averaged over the current sheet center region, $z \in [-3, 3]d_i$) with $j_{||}(t)$ derived at the virtual MMS position. This comparison simulates the spacecraft measurements of $v_x$ and $j_{||}$ for different events.

Figure 4h shows that a positive correlation between $v_x$ and $j_{||}$ indeed exists, reproducing the main feature of the observations in Figure 3. Careful inspection of the 2-D $j_{||}(x, z)$ distribution reveals that the field-aligned currents observed around the virtual MMS position (at the plasma sheet boundary) are most likely generated at the reconnection region. These currents are a natural continuation of the Hall current system around reconnection (see, e.g., review by Paschmann et al., 2013, and references therein). There is also a second field-aligned current system related to the earthward propagating plasma flow and dipolarization front (see Figure 4c and Birn et al., 1999). We cannot exclude the possibility that field-aligned currents captured by MMS in the plasma sheet boundary are partially due to this system. However, the field-aligned current polarity in MMS

observations is mostly negative below the equatorial plane ($B_x < 0$), as in simulations (Figure 4(c)), suggesting that we mainly deal with currents originated from the reconnection region.

The agreement between observations (Figures 2 and 3) and simulations (Figure 4) suggests that due to the conjugation of MMS and ARTEMIS, based on conditions just prior to reconnection (before the dipolarization detected by MMS), the subsequent magnetic reconnection region affects the near-Earth boundary layer currents and midtail tailward flows in a way consistent with their generation by a common driver. This confirms our hypothesis that the good correlation between observed field-aligned current intensity and average tailward plasma flows is likely due to a common origin, magnetic reconnection between them.

## 4. Discussion and Conclusions

Our data set demonstrates that MMS/ARTEMIS conjugations, which can often be established in the magnetotail, provides us with a unique opportunity to investigate the relationship between equatorial and high-latitude magnetotail dynamics on a global scale. There are two interesting problems to be considered in further studies using such techniques. First, high-resolution electric and magnetic field measurements by the MMS spacecraft give us a chance to investigate energy transport (Poynting flux) and its relation to the equatorial plasma distribution for selected MMS/ARTEMIS conjunctions. Such field-aligned energy flux plays an important role in driving the aurora (see, e.g., Angelopoulos et al., 2002; Lysak & Song, 2003, and references therein). Second, MMS observations at the plasma sheet boundary sometimes include high-resolution plasma measurements (e.g., Nakamura et al., 2017; Stawarz et al., 2017). The correlation between such MMS measurements with ARTEMIS observations can reveal the kinetics of field-aligned current generation beyond the standard fluid picture of large-scale field-aligned current systems (see reviews by Ganushkina et al., 2015; Kepko et al., 2014, and references therein).

In summary, by combining MMS observations at the plasma sheet boundary, equatorial ARTEMIS observations, and PIC simulations of magnetotail magnetic reconnection, we have demonstrated the following:

- The field-aligned currents observed near the plasma sheet boundary by MMS in the near-Earth magnetotail are likely generated by near-Earth magnetic reconnection. As these currents are not correlated with magnitudes of earthward plasma flows measured by ARTEMIS, distant magnetotail reconnection (beyond the lunar orbit) likely does not contribute significantly to the development of the field-aligned current system.
- The observed correlation between the tailward plasma flow magnitude at ARTEMIS and the field-aligned current intensity at the near-Earth plasma sheet boundary at MMS suggests that these field-aligned currents arise from the reconnection region and their intensity is determined by the same energy release process as are equatorial plasma flow magnitudes.
- As MMS and ARTEMIS were likely within the same flux tube (by virtue of event selection, exhibiting similar ion temperature/density at the two locations) before reconnection onset, they likely become disconnected by magnetic field line reconnection near the time of MMS dipolarization and observe the consequences (field-aligned currents and plasma flows) of the same driver on opposite sides of the reconnection region.

Although the correlation between intensities of currents and flows can be explained by their common origin, MMS and ARTEMIS may find themselves again on the same flux tubes after the reconnection region retreats tailward, past ARTEMIS. At such times, the field-aligned current system could have a complicated 3-D configuration, different from the simple 2-D structure assumed in this study (e.g., Nakamura et al., 2018, and references therein). These ideas require further observational and simulation investigations, which can reveal the details of magnetotail reconfiguration after near-Earth reconnection.

**Acknowledgments**
We thank J. Burch and R. Torbert for leading the MMS observations. We also thank M. Andriopoulou (IWF Graz) for help with MMS ASPOC data. The Space Physics Environment Data Analysis Software (SPEDAS, spedas.org) was used for data processing. We acknowledge NASA contract NAS5-02099 for use of data from the THEMIS Mission and the NASA Advanced Supercomputing (NAS) Division at Ames Research Center for the provision of computing resources. The research of PLP was supported by NASA grant NNX14AF70G. V. A. credits NASA MMS IDS grant NNX08AO83G for support. R. N. and S. W. acknowledged support of Austrian Science Funds (FWF)I2016-N20. We would like to thank the following people, specifically: C. W. Carlson and J. P. McFadden for use of ESA data, D.E. Larson and R.P. Lin for use of SST data, and K. H. Glassmeier, U. Auster and W. Baumjohann for the use of FGM data provided under the lead of the Technical University of Braunschweig and with financial support through the German Ministry for Economy and Technology and the German Aerospace Center (DLR) under contract 50 OC 0302. ARTEMIS and MMS data are downloaded at http://themis.ssl.berkeley.edu/ and https://lasp.colorado.edu/mms/sdc/. The PIC simulation data are available from pritchet@physics.ucla.edu.

## References

Andriopoulou, M., Nakamura, R., Torkar, K., Baumjohann, W., Torbert, R. B., Lindqvist, P.-A., et al. (2016). Study of the spacecraft potential under active control and plasma density estimates during the MMS commissioning phase. *Geophysical Research Letters*, *43*, 4858–4864. https://doi.org/10.1002/2016GL068529

Angelopoulos, V. (2011). The ARTEMIS mission. *Space Science Reviews*, *165*, 3–25. https://doi.org/10.1007/s11214-010-9687-2

Angelopoulos, V., Chapman, J. A., Mozer, F. S., Scudder, J. D., Russell, C. T., Tsuruda, K., et al. (2002). Plasma sheet electromagnetic power generation and its dissipation along auroral field lines. *Journal of Geophysical Research*, *107*(A8), 1181. https://doi.org/10.1029/2001JA900136

Angelopoulos, V., McFadden, J. P., Larson, D., Carlson, C. W., Mende, S. B., Frey, H., et al. (2008). Tail reconnection triggering substorm onset. *Science*, *321*, 931–935. https://doi.org/10.1126/science.1160495

Angelopoulos, V., Runov, A., Zhou, X. Z., Turner, D. L., Kiehas, S. A., Li, S. S., & Shinohara, I. (2013). Electromagnetic energy conversion at reconnection fronts. *Science*, *341*, 1478–1482. https://doi.org/10.1126/science.1236992

Artemyev, A. V., Angelopoulos, V., Hietala, H., Runov, A., & Shinohara, I. (2017). Ion density and temperature profiles along ($X_{GSM}$) and across ($Z_{GSM}$) the magnetotail as observed by THEMIS, Geotail, and ARTEMIS. *Journal of Geophysical Research: Space Physics*, *122*, 1590–1599. https://doi.org/10.1002/2016JA023710

Auster, H. U., Glassmeier, K. H., Magnes, W., Aydogar, O., Baumjohann, W., Constantinescu, D., et al. (2008). The THEMIS fluxgate magnetometer. *Space Science Reviews*, *141*, 235–264. https://doi.org/10.1007/s11214-008-9365-9

Baker, D. N., Pulkkinen, T. I., Angelopoulos, V., Baumjohann, W., & McPherron, R. L. (1996). Neutral line model of substorms: Past results and present view. *Journal of Geophysical Research*, *101*(A6), 12,975–13,010. https://doi.org/10.1029/95JA03753

Birn, J., & Hesse, M. (2013). The substorm current wedge in MHD simulations. *Journal of Geophysical Research: Space Physics*, *118*, 3364–3376. https://doi.org/10.1002/jgra.50187

Birn, J., Hesse, M., Haerendel, G., Baumjohann, W., & Shiokawa, K. (1999). Flow braking and the substorm current wedge. *Journal of Geophysical Research*, *104*(A9), 19,895–19,904. https://doi.org/10.1029/1999JA900173

Burch, J. L., Moore, T. E., Torbert, R. B., & Giles, B. L. (2016). Magnetospheric Multiscale overview and science objectives. *Space Science Reviews*, *199*, 5–21. https://doi.org/10.1007/s11214-015-0164-9

Chaston, C. C., Bonnell, J. W., & Salem, C. (2014). Heating of the plasma sheet by broadband electromagnetic waves. *Geophysical Research Letters*, *41*, 8185–8192. https://doi.org/10.1002/2014GL062116

Dunlop, M. W., Balogh, A., Glassmeier, K.-H., & Robert, P. (2002). Four-poin Cluster application of magnetic field analysis tools: The Curlometer. *Journal of Geophysical Research*, *107*(A11), 1384. https://doi.org/10.1029/2001JA005088

Eastwood, J. P., Phan, T. D., Drake, J. F., Shay, M. A., Borg, A. L., Lavraud, B., & Taylor, M. G. G. T. (2013). Energy partition in magnetic reconnection in Earth's magnetotail. *Physical Review Letters*, *110*(22), 225001. https://doi.org/10.1103/PhysRevLett.110.225001

Ergun, R. E., Tucker, S., Westfall, J., Goodrich, K. A., Malaspina, D. M., Summers, D., et al. (2016). The axial double probe and fields signal processing for the MMS mission. *Space Science Reviews*, *199*, 167–188. https://doi.org/10.1007/s11214-014-0115-x

Ganushkina, N. Y., Liemohn, M. W., Dubyagin, S., Daglis, I. A., Dandouras, I., De Zeeuw, D. L., et al. (2015). Defining and resolving current systems in geospace. *Annales Geophysicae*, *33*, 1369–1402. https://doi.org/10.5194/angeo-33-1369-2015

Kepko, L., McPherron, R. L., Amm, O., Apatenkov, S., Baumjohann, W., Birn, J., et al. (2014). Substorm current wedge revisited. *Space Science Reviews*, *190*, 1–46. https://doi.org/10.1007/s11214-014-0124-9

Lembege, B., & Pellat, R. (1982). Stability of a thick two-dimensional quasineutral sheet. *Physics of Fluids*, *25*, 1995–2004. https://doi.org/10.1063/1.863677

Li, S.-S., Angelopoulos, V., Runov, A., & Kiehas, S. A. (2014). Azimuthal extent and properties of midtail plasmoids from two-point ARTEMIS observations at the Earth-Moon Lagrange points. *Journal of Geophysical Research: Space Physics*, *119*, 1781–1796. https://doi.org/10.1002/2013JA019292

Lu, S., Artemyev, A. V., Angelopoulos, V., Lin, Y., & Wang, X. Y. (2017). The ion temperature gradient: An intrinsic property of Earth's magnetotail. *Journal of Geophysical Research: Space Physics*, *122*, 8295–8309. https://doi.org/10.1002/2017JA024209

Lysak, R. L., & Song, Y. (2003). Kinetic theory of the Alfvén wave acceleration of auroral electrons. *Journal of Geophysical Research: Space Physics*, *108*, 8005. https://doi.org/10.1029/2002JA009406

McFadden, J. P., Carlson, C. W., Larson, D., Ludlam, M., Abiad, R., Elliott, B., & Turin, P. (2008). Th THEMIS ESA plasma instrument and in-flight calibration. *Space Science Reviews*, *141*, 277–302. https://doi.org/10.1007/s11214-008-9440-2

Nagai, T., Shinohara, I., Zenitani, S., Nakamura, R., Nakamura, T. K. M., Fujimoto, M., et al. (2013). Three-dimensional structure of magnetic reconnection in the magnetotail from Geotail observations. *Journal of Geophysical Research: Space Physics*, *118*, 1667–1678. https://doi.org/10.1002/jgra.50247

Nakamura, R., Baumjohann, W., Mouikis, C., Kistler, L. M., Runov, A., Volwerk, M., et al. (2004). Spatial scale of high-speed flows in the plasma sheet observed by Cluster. *Geophysical Research Letters*, *31*, L09804. https://doi.org/10.1029/2004GL019558

Nakamura, R., Nagai, T., Birn, J., Sergeev, V. A., Le Contel, O., Varsani, A., et al. (2017). Near-Earth plasma sheet boundary dynamics during substorm dipolarization. *Earth, Planets and Space*, *69*, 129. https://doi.org/10.1186/s40623-017-0707-2

Nakamura, R., Varsani, A., Genestreti, K. J., Le Contel, O., Nakamura, T., Baumjohann, W., et al. (2018). Multiscale currents observed by MMS in the flow braking region. *Journal of Geophysical Research: Space Physics*, *123*, 1260–1278. https://doi.org/10.1002/2017JA024686

Paschmann, G., Øieroset, M., & Phan, T. (2013). In-situ observations of reconnection in space. *Space Science Reviews*, *178*, 385–417. https://doi.org/10.1007/s11214-012-9957-2

Pritchett, P. L. (2015). Structure of exhaust jets produced by magnetic reconnection localized in the out-of-plane direction. *Journal of Geophysical Research: Space Physics*, *120*, 592–608. https://doi.org/10.1002/2014JA020795

Pritchett, P. L., & Coroniti, F. V. (1998). Interchange instabilities and localized high-speed flows in the convectively-driven near-Earth plasma sheet. In S. Kokubun & Y. Kamide (Eds.), *Substorms-4, Astrophysics and Space Science Library* (Vol. 238, pp. 443). https://doi.org/10.1007/978-0-7923-5465-993

Pritchett, P. L., Coroniti, F. V., & Decyk, V. K. (1996). Three-dimensional stability of thin quasi-neutral current sheets. *Journal of Geophysical Research*, *101*(A12), 27,413–27,430. https://doi.org/10.1029/96JA02665

Pritchett, P. L., Coroniti, F. V., Pellat, R., & Karimabadi, H. (1991). Collisionless reconnection in two-dimensional magnetotail equilibria. *Journal of Geophysical Research*, *96*(A7), 11,523–11,538. https://doi.org/10.1029/91JA01094

Pritchett, P. L., & Runov, A. (2017). The interaction of finite-width reconnection exhaust jets with a dipolar magnetic field configuration. *Journal of Geophysical Research: Space Physics*, *122*, 3183–3200. https://doi.org/10.1002/2016JA023784

Russell, C. T., Anderson, B. J., Baumjohann, W., Bromund, K. R, Dearborn, D., Fischer, D., et al. (2016). The Magnetospheric Multiscale magnetometers. *Space Science Reviews*, *199*, 189–256. https://doi.org/10.1007/s11214-014-0057-3

Stawarz, J. E., Eastwood, J. P., Varsani, A., Ergun, R. E., Shay, M. A., Nakamura, R., et al. (2017). Magnetospheric Multiscale analysis of intense field-aligned Poynting flux near the Earth's plasma sheet boundary. *Geophysical Research Letters*, *44*, 7106–7113. https://doi.org/10.1002/2017GL073685

Torbert, R. B., Russell, C. T., Magnes, W., Ergun, R. E., Lindqvist, P.-A., Le Contel, O., et al. (2016). The FIELDS instrument suite on MMS: Scientific objectives, measurements, and data products. *Space Science Reviews*, *199*, 105–135. https://doi.org/10.1007/s11214-014-0109-8

Tyler, E., Cattell, C., Thaller, S., Wygant, J., Gurgiolo, C., Goldstein, M., & Mouikis, C. (2016). Partitioning of integrated energy fluxes in four tail reconnection events observed by Cluster. *Journal of Geophysical Research: Space Physics*, *121*, 11,798–11,825. https://doi.org/10.1002/2016JA023330

Varsani, A., Nakamura, R., Sergeev, V. A., Baumjohann, W., Owen, C. J., Petrukovich, A. A., et al. (2017). Simultaneous remote observations of intense reconnection effects by DMSP and MMS spacecraft during a storm time substorm. *Journal of Geophysical Research: Space Physics*, *122*, 10,891–10,909. https://doi.org/10.1002/2017JA024547

Wygant, J. R., Keiling, A., Cattell, Lysak, R. L., Temeren, M., Mozer, F. S., et al. (2002). Evidence for kinetic Alfvén waves and parallel electron energization at 4-6 $R_E$ altitudes in the plasma sheet boundary layer. *Journal of Geophysical Research*, *107*(A8), 1201. https://doi.org/10.1029/2001JA900113

Young, D. T., Burch, J. L, Gomez, R. G., De Los Santos, A., Miller, G. P., Wilson, P., et al. (2016). Hot plasma composition analyzer for the Magnetospheric Multiscale mission. *Space Science Reviews*, *199*, 407–470. https://doi.org/10.1007/s11214-014-0119-6